GS-14

Diagenesis of the Lower Silurian Ekwan River and Attawapiskat formations, Hudson Bay Lowland, northern Manitoba (parts of NTS 54B, F, G)

by L.A. Eggie[1], E. Pietrus[2], A. Ramdoyal[2] and N. Chow[1]

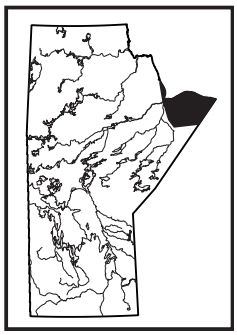

Eggie, L.A., Pietrus, E., Ramdoyal, A. and Chow, N. 2014: Diagenesis of the Lower Silurian Ekwan River and Attawapiskat formations, Hudson Bay Lowland, northern Manitoba (parts of NTS 54B, F, G); *in* Report of Activities 2014, Manitoba Mineral Resources, Manitoba Geological Survey, p. 161–171.

Summary

The Lower Silurian Ekwan River and Attawapiskat formations in the Hudson Bay Lowland of northern Manitoba share a similar diagenetic history, which includes alteration in the synsedimentary marine, burial and late-stage meteoric diagenetic realms. Marine diagenesis was typified by precipitation of nonferroan micrite, radial-fibrous, and radiaxial-fibrous to radiaxial-blocky cements. Burial diagenesis produced a variety of features, including dolomicrite; anhydrite laths; flattened and 'canoe'-shaped peloids, and fitted-grain fabrics; nonferroan blocky to bladed calcite cements; planar and nonplanar dolomites; fluorite and chalcedony; and numerous dissolution features, including corroded calcite cements and vuggy and mouldic porosity, generated by at least two stages of dissolution. Anhydrite calcitization, dedolomitization, and a third stage of dissolution, generating intracrystalline and mouldic porosity, are tentatively attributed to late-stage meteoric diagenesis related to extensive subaerial exposure of the Hudson Bay Platform during the late Silurian to early Devonian. The sabkha and seepage-reflux dolomitization models are proposed as the most likely mechanisms to explain dolomitization in both the Ekwan River and Attawapiskat formations.

A better understanding of the diagenetic history of these units provides a strong basis for evaluating the reservoir potential of the two formations. Notably, multiple dissolution and dolomitization events, which generated high secondary porosity, and the lack of late-stage cementation to occlude this porosity resulted in better reservoir qualities with progressive diagenesis. Oil staining was observed in one interval of lithofacies E of the Ekwan River Formation, indicating that oil passed through this formation in the past and suggesting that there may be trapped oil accumulations in other areas of the Hudson Bay Basin.

Introduction

The Lower Silurian Ekwan River Formation and overlying Attawapiskat Formation of the Hudson Bay Basin are carbonate-dominated successions interpreted to have been deposited in peritidal environments (Lavoie et al., 2013; Pietrus, 2013; Ramdoyal et al., 2013). These formations show similar diagenetic features that are considered to reflect alteration in the marine, burial and meteoric diagenetic realms. Both units are considered to have good reservoir potential and have been targeted by the Geo-mapping for Energy and Minerals (GEM) program (Hamblin, 2008; Lavoie et al., 2013). Detailed investigation of the diagenetic controls on the reservoir qualities of these units is warranted.

The purpose of this study was to utilize select samples of the Ekwan River and Attawapiskat formations that were originally studied by Ramdoyal (2012) and Pietrus (2013), with the goal of re-examining the diagenetic features in these units and interpreting and comparing their paragenetic sequences.

Geological setting

In the Hudson Bay Lowland in northern Manitoba, the preserved succession of Upper Ordovician to Lower Devonian strata of the Hudson Bay Basin overlies Precambrian crystalline basement (Lavoie et al., 2013). Strata dip generally toward the northeast and are the erosional remnants of an extensive sedimentary succession that once covered the Canadian Shield. Good outcrop exposures are limited to the Hudson Bay coast and along river valleys; hence, key information is provided primarily by exploratory petroleum wells, stratigraphic testholes, and mineral exploration and geotechnical holes (summarized in Lavoie et al., 2013). For the Silurian succession, cores from three exploration wells, Merland et al. Whitebear Creek Prov. (WBC), Sogepet Aquitaine Kaskattama Prov. No. 1 (KTC), and Houston Oils et al. Comeault Prov. No. 1 (CT) are particularly useful. Figure GS-14-1 shows the Silurian to Lower Devonian stratigraphy of the HBL and Figure GS-12-2 (Nicolas et al., GS-12, this volume) shows the well locations.

The Silurian succession in the Hudson Bay Lowland in Manitoba, in ascending order, consists of 1) the Severn River Formation, which is 135–241 m thick and composed mainly of interbedded laminated, nodular and burrow-mottled lime mudstone to wackestone; 2) the Ekwan River Formation, which is 42–84 m thick and primarily

[1] Department of Geological Sciences, University of Manitoba, 125 Dysart Road, Winnipeg, MB R3T 2N2
[2] formerly of Department of Geological Sciences, University of Manitoba, 125 Dysart Road, Winnipeg, MB R3T 2N2

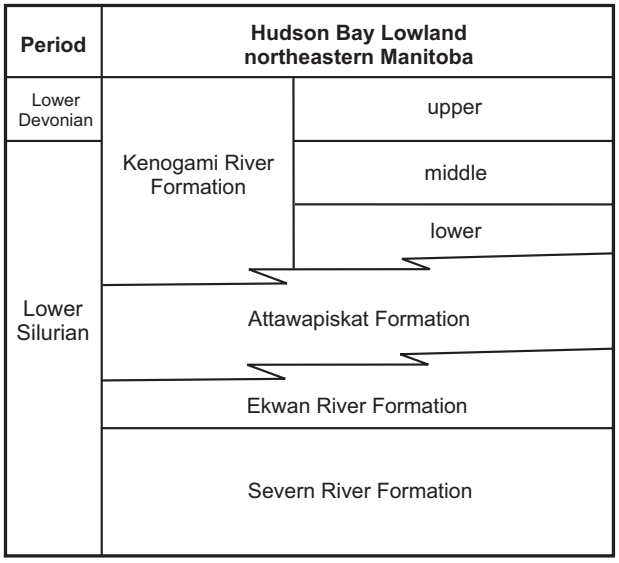

Figure GS-14-1: *Silurian to Lower Devonian stratigraphic column of the Hudson Bay Lowland, northeastern Manitoba (Ramdoyal et al., 2013).*

skeletal wackestone to packstone; and 3) the Attawapiskat Formation, which is 37–65 m thick and composed of stromatoporoid boundstone, skeletal mudstone to wackestone, and peloidal wackestone to bindstone (Lavoie et al., 2013; Pietrus, 2013; Ramdoyal et al., 2013). This succession correlates to the Interlake Group in the Williston Basin, but more detailed correlations are difficult to make.

Ekwan River Formation lithofacies

The Ekwan River Formation in the WBC, KTC and CT cores was subdivided by Pietrus (2013) into three lithofacies associations, which are composed of seven lithofacies. These lithofacies associations are interpreted to represent an arid peritidal setting within an overall rimmed-shelf environment. The subtidal lithofacies association (LA1) is composed of two lithofacies: A, nodular to mottled stromatoporoid-coral floatstone; and B, nodular to mottled skeletal wackestone. This lithofacies association is interpreted to have been deposited in open subtidal conditions between storm and fair-weather wave base. The intertidal lithofacies association (LA2) comprises four lithofacies: C, intraclast floatstone; D, peloidal wackestone; E, laminated dolomudstone; and F, laminated lime mudstone. This lithofacies association is interpreted to have been deposited in low-energy intertidal environments with rare storm events. The supratidal lithofacies association (LA3) consists of only one lithofacies: G, nodular anhydrite. It is interpreted to have been deposited in a sabkha environment and was only observed at the base of the KTC core.

Lavoie et al. (2013) modified this previous work and assigned lithofacies A to D to the subtidal lithofacies association (LA1) and lithofacies E and F to the intertidal lithofacies association (LA2). They also considered lithofacies G at the base of the KTC core to be part of the underlying Severn River Formation.

For this study, the definitions and interpretations of lithofacies and lithofacies associations of Pietrus (2013) were used.

Attawapiskat Formation lithofacies

Ten lithofacies have been recognized in the Attawapiskat Formation, in the WBC, KTC and CT cores, and are grouped into three lithofacies associations (Ramdoyal, 2012; Ramdoyal et al., 2013). These lithofacies associations are interpreted to have been deposited in a rimmed, shallow, carbonate shelf. The subtidal lithofacies association (LA1) is composed of eight lithofacies: A, mottled to nodular skeletal wackestone; B, stromatoporoid-coral framestone; C, stromatoporoid-coral rudstone; D, peloidal-intraclastic wackestone to grainstone; E, skeletal mudstone to wackestone; F, peloidal intraclastic bindstone; G, interbedded skeletal wackestone and intraclastic rudstone; and H, graded oolitic grainstone to wackestone. The lithofacies association is interpreted to have been deposited in a variety of environments in the inner shelf setting. Conditions ranged from low to high energy, and depositional environments include patch reefs (lithofacies B) and reef flanks (lithofacies C). The intertidal lithofacies association (LA2) is composed of only one lithofacies: I, laminated skeletal mudstone to wackestone. This lithofacies is interpreted to have been deposited in an overall low-energy tidal-flat setting. The supratidal lithofacies association (LA3) is composed of only one lithofacies: J, laminated dolostone; it is interpreted to represent the shallowest portion of a tidal flat.

Methodology

Transmitted-light microscopy

Twenty-five representative thin sections (12 from the Ekwan River Formation and 13 from the Attawapiskat Formation), selected from those previously made for projects of Ramdoyal (2012) and Pietrus (2013), were examined using a Nikon Optiphot-Pol microscope. These thin sections had been stained with Alizarin Red S and potassium ferricyanide, following the technique outlined in Dickson (1965), to distinguish calcite from dolomite and to identify ferroan carbonate minerals. Photomicrographs were taken with a Nikon DS-L2 camera attachment and oriented with the upping direction at the top of each photo. Porosity was described using the terminology of Choquette and Pray (1970); the term ‘pinpoint porosity’ is used to refer to dissolution-formed pores <0.25 mm diameter, whereas ‘vuggy porosity’ is used to describe dissolution-formed pores >0.25 mm diameter. Dolomite

textures were named using the classification system of Sibley and Gregg (1987). Neomorphic textures of the micrite matrix were described using the terminology of Folk (1965).

Cathodoluminescence and epifluorescence microscopy

Cathodoluminescence (CL) microscopy was completed on four polished thin sections from the Ekwan River Formation and six polished thin sections from the Attawapiskat Formation using a Technosyn Cold Cathodoluminescence (model 8200 MkII) system, attached to a Nikon Optiphot-Pol microscope with a Nikon DS-U2 camera. Zoning in calcite cements and dolomites and replacement textures were described and photographed. Epifluorescence microscopy of three thin sections from the Ekwan River Formation and three thin sections from the Attawapiskat Formation was accomplished using a Nikon Optiphot-Pol microscope fitted with a mercury lamp and blue-violet filter block (436 nm wavelength); photomicrographs were taken using a Nikon DS-L2 camera attachment. Features identified and described using this technique include calcite cement and dolomite zonation and the presence of oil staining.

Diagenetic features

The general characteristics of the major diagenetic features in the Ekwan River and Attawapiskat formations in the WBC, KTC and CT cores are described below; more information about each feature is provided in Table GS-14-1.

Calcite cements

Micrite cement

Micrite cement is rare within subtidal lithofacies of both the Ekwan River and Attawapiskat formations. This cement is microcrystalline and typically occurs either as linings of intraparticle porosity within bivalve shells or as rims on brachiopod shell fragments, crinoids and other allochems.

Isopachous, radial-fibrous, calcite cement

Nonferroan, radial-fibrous, calcite cement is rare in both formations, occurring primarily in subtidal lithofacies. It was observed lining the interior of a large gastropod shell and articulated thin bivalve shells. This cement is nonluminescent.

Radiaxial-fibrous to radiaxial-blocky calcite cement

Nonferroan, radiaxial-fibrous to radiaxial-blocky, calcite cement was rarely observed in subtidal and intertidal lithofacies. These cements are characterized by sweeping extinction and the blocky crystals appear to be due to recrystallization of fibrous crystals (cf. Kendall and Tucker, 1973). The cements occur as isopachous linings in bivalve shells and overgrowths on brachiopod shells, which commonly terminate in micrite matrix. A single occurrence of inclusion-rich botryoidal bundles was observed partially filling the interior of a single, large gastropod shell. Radiaxial-fibrous and radiaxial-blocky calcite is nonluminescent but commonly exhibits nonfluorescent centres and dull-fluorescent crystal terminations.

Syntaxial calcite overgrowths

Nonferroan syntaxial calcite overgrowths are very common throughout the Ekwan River and Attawapiskat formations. These overgrowths are primarily observed on crinoids or other echinoderm fragments, but rarely occur on brachiopod fragments, and partially to fully fill interparticle and intraparticle pore space (Figure GS-14-2). These cements are nonluminescent to simply zoned with nonluminescent cores and dull terminations. They rarely exhibit simple to oscillatory zonation of nonfluorescent and dull-fluorescent sections.

Isopachous, blocky to bladed, calcite cement

Isopachous, nonferroan, bladed to blocky, calcite cement is one of the most common cements in both formations. Shorter, blocky crystals typically have rounded crystal terminations, whereas longer, bladed crystals generally have scalenohedral to irregular terminations (Figure GS-14-2). The cement partially to fully lines intraparticle, interparticle, fenestral and fracture pore spaces. It was also rarely observed in shelter porosity beneath brachiopod shells. This cement is typically nonluminescent to dull luminescent with nonluminescent patches; it also exhibits common nonfluorescence to patchy dull epifluorescence and rare simple zonation of dull cores and bright terminations.

Coarse-mosaic calcite cement

Nonferroan, coarse-mosaic, calcite cement is very common in the Ekwan River and Attawapiskat formations. It partially or fully fills interparticle, intraparticle, vuggy and fracture pore spaces (Figure GS-14-2). The crystals form an interlocking texture with irregular crystal-to-crystal boundaries being common and triple junctions being rare. Crystal margins are rarely corroded when adjacent to open interparticle or intercrystalline pores. Coarse-mosaic calcite crystals were rarely observed to overgrow, and to be optically continuous with, radiaxial-fibrous calcite cement. Coarse-mosaic calcite cement is nonluminescent to moderately luminescent, with rare crystal zonation of dull cores and bright rims. It typically exhibits epifluorescence ranging from dull fluorescent

Table GS-14-1: Diagenetic features of the Ekwan River and Attawapiskat formations. Lithofacies descriptions are provided in the text.

Diagenetic features	Ekwan River Formation		Attawapiskat Formation	
	Size	Occurrence (lithofacies)	Size	Occurrence (lithofacies)
Micritized allochems	50–100% of allochems	Common in all fossiliferous facies	Envelopes to 100% micritized	D, E, G, H and I
Micrite cement	8–32 µm thick rims/ linings	Rare in all fossiliferous facies	Same as Ekwan River Fm. occurrences	Rare in C and G
Isopachous radial-fibrous calcite cement	~80 µm long	C and D	96–160 µm long	B and D
Radiaxial-fibrous to radiaxial-blocky calcite cement	70–4500 µm long	C, D and F	120–210 µm long	D
Syntaxial calcite cement	40–800 µm size	All crinoidal lithofacies	20–1300 µm size	All crinoidal lithofacies
Isopachous blocky to bladed calcite cement	4–80 µm long	Very common; all lithofacies except E and G	4–180 µm long	Very common; all fossiliferous lithofacies
Coarse-mosaic calcite cement	20–500 µm size	Very common; all fossiliferous lithofacies	24–1560 µm size	Very common; all lithofacies except J
Dolomicrite	Aphanocrystalline to 30 µm size	Most in E	Aphanocrystalline to 40 µm size	J
Nonplanar dolomite	12–28 µm size	Very rare; E	24–40 µm size	Rare; J
Planar dolomite	4–80 µm size	All lithofacies except C and G	8–120 µm size	D, I and J
Mimetic dolomite	140–300 µm size	A, B and F	Not observed	Not observed
Dedolomite	8–20 µm size	A	48–72 µm size	B, D and I
Authigenic pyrite	4–24 µm size crystals; 24–200 µm diameter framboids	A, C, D, E and F	4–220 µm size crystals (rare framboids)	All lithofacies except B, H and I
Anhydrite ‘ghosts’	440–2400 µm long	C and D	80–1800 µm long	B, C and D
Fluorite	Not observed	Not observed	12–96 µm diameter	C and G
Chalcedony	0.1–2.3 mm diameter nodules	A and D	0.08–0.38 mm size nodules	G
Microspar/pseudospar	4–120 µm	Micritic lithofacies	2–36 µm	All micritic lithofacies
Pinpoint porosity	<250 µm	Micritic lithofacies	<250 µm	B, E, G, I
Vuggy porosity	>250 µm	E and B	<250 µm	A and D
Mouldic porosity	Large range	Fossiliferous lithofacies	Large range	Fossiliferous lithofacies
Intercrystalline porosity	<80 µm	Most lithofacies	<120 µm	Most lithofacies
Intracrystalline porosity	<80 µm	A	Not observed	Not observed
Fractures	16–40 µm wide	A, B and F	24–130 µm wide	D, F, G and I
Compacted grains	N/A	C and D	N/A	H
Microstylolites/stylolites	N/A	B and F	N/A	A and D

and nonfluorescent patches to simple zonation with dull inner zones and moderately bright outer zones.

Dolomite

Dolomicrite

Nonferroan dolomicrite occurs in intertidal and supratidal lithofacies of the Ekwan River and Attawapiskat formations, where it commonly composes the majority of the lithofacies. Dolomicrite exhibits uniform, dull to moderate luminescence and uniform, dull to bright fluorescence.

Nonplanar dolomite

Nonferroan nonplanar (typically anhedral) dolomite was only observed in the intertidal lithofacies of the Ekwan River Formation and the supratidal lithofacies of the Attawapiskat Formation. It typically occurs as patches of tightly packed crystals, which are inclusion rich and exhibit uniform, dull luminescence and dull fluorescence.

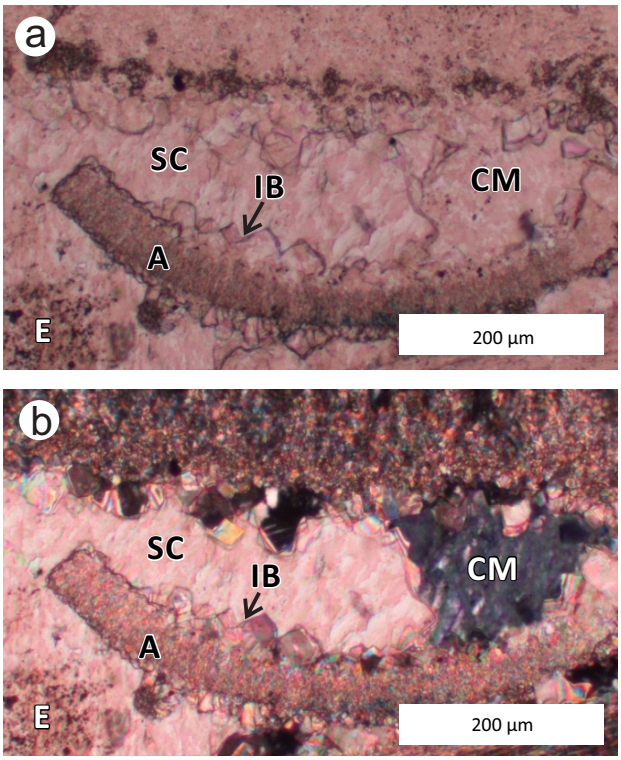

Figure GS-14-2: *Photomicrographs of isopachous, nonferroan, blocky to bladed, calcite cement (IB) on an arthropod shell (A), with nonferroan coarse-mosaic calcite cement (CM), and nonferroan syntaxial calcite cement (SC) overgrowing an echinoderm fragment (E). Photomicrograph* ***a)*** *in plane-polarized light and* ***b)*** *in cross-polarized light. Sample from lithofacies A, Ekwan River Formation, Houston Oils et al. Comeault Prov. No. 1 well at 178.98 m (587.2 ft.). See Figure GS-12-2 (Nicolas et al., GS-12, this volume) for well location.*

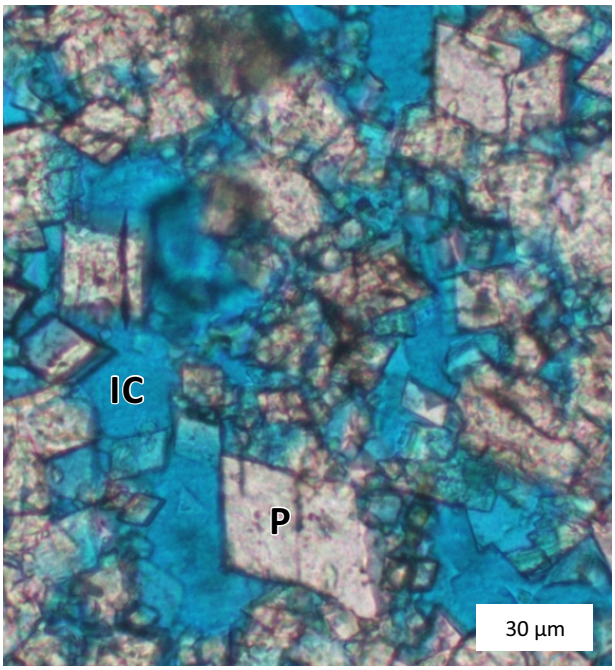

Figure GS-14-3: *Photomicrograph of nonferroan dolomite (P) with dominantly euhedral crystal textures. Blue epoxy highlights intercrystalline porosity (IC). Plane-polarized light. Sample from lithofacies E, Ekwan River Formation, Sogepet Aquitaine Kaskattama Prov. No. 1 well at 395.11 m (1296.3 ft.). See Figure GS-12-2 (Nicolas et al., GS-12, this volume) for well location.*

Planar dolomite

Nonferroan planar dolomite is common in most lithofacies of the Ekwan River Formation, but is relatively minor in the Attawapiskat Formation. It is dominated by either subhedral crystal textures (planar-s) or euhedral crystal textures (planar-e; Figure GS-14-3), with a minor proportion of anhedral crystals. Planar dolomite commonly occurs within micrite matrix, replacing coarse-mosaic cement or rarely concentrated along dissolution seams. Rhombs are commonly nonzoned and inclusion poor. Planar-s dolomite is typically smaller in crystal size than planar-e dolomite. Overall, planar dolomite is more loosely packed than nonplanar dolomite, and is commonly associated with moderate amounts (5–10%) of intercrystalline porosity. Planar-s and planar-e dolomite typically exhibit uniform, dull to moderate luminescence, with rare zoned rhombs having bright cores and dull rims. Dolomite rhombs also typically exhibit uniform, dull fluorescence with rare, large rhombs having bright cores and dull rims.

Mimetic dolomite

Nonferroan mimetic dolomite is rarely present in the Ekwan River Formation. Mimetic dolomite partially replaces crinoid ossicles and small proportions of laminar brachiopod shell fragments.

Dedolomite

Dedolomite was rarely observed in several lithofacies in each formation. It consists of nonferroan calcite, which partially to fully replaced the cores and rarely the rims of planar-e and planar-s dolomite rhombs (Figure GS-14-4). Mouldic or vuggy porosity occurs within and adjacent to some dedolomite crystals.

Anhydrite 'ghosts'

Anhydrite ghosts are anhydrite laths that have been either replaced by microspar and/or undergone dissolution with the resulting moulds filled by coarse-mosaic calcite cement (Figure GS-14-5). They are rare in the Ekwan River Formation, and slightly more common in the Attawapiskat Formation. They commonly cut across and replace matrix, allochems and radiaxial-fibrous calcite cement. Anhydrite laths that cut across allochems are now moulds partially filled with isopachous blocky to bladed

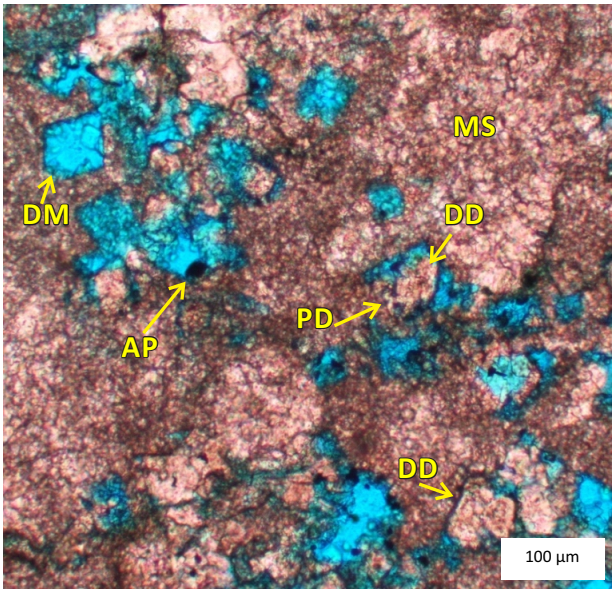

Figure GS-14-4: *Photomicrograph of nonferroan dedolomite (DD), partially dissolved dedolomite (PD), and dolomite moulds (DM) within micrite and microspar matrix (MS). Mouldic porosity is highlighted by blue epoxy. Small black grains are authigenic pyrite (AP). Plane-polarized light. Sample from lithofacies D, Attwapiskat Formation, Sogepet Aquitaine Kaskattama Prov. No. 1 well at 329.79 m (1082 ft.). See Figure GS-12-2 (Nicolas et al., GS-12, this volume) for well location.*

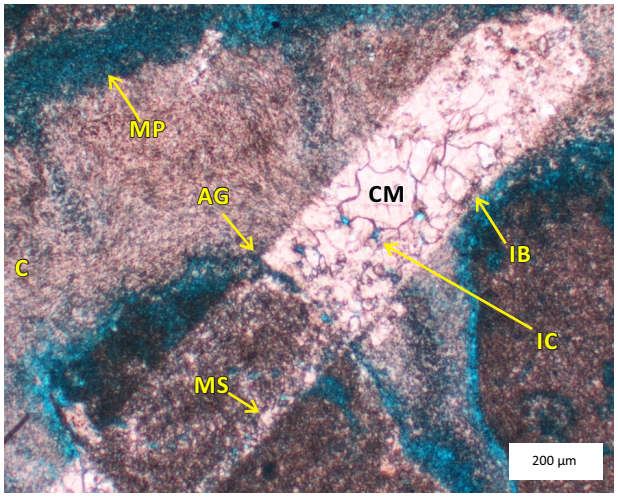

Figure GS-14-5: *Photomicrograph of anhydrite 'ghost' (AG). Section crosscutting rugose coral (C) is now filled with isopachous, nonferroan, blocky to bladed, calcite cement (IB) and nonferroan, coarse-mosaic, calcite cement (CM); section crosscutting micrite matrix is partially replaced by microspar (MS). Blue epoxy highlights mouldic porosity (MP) and intercrystalline (IC) porosity. Plane-polarized light. Sample from lithofacies C, Attawapiskat Formation, Merland et al. Whitebear Creek Prov. well at 42.46 m (139.3 ft.). See Figure GS-12-2 (Nicolas et al., GS-12, this volume) for well location.*

and coarse-mosaic calcite cements, whereas laths that occur in micrite are commonly replaced by microspar.

Fluorite and chalcedony

Very fine to medium crystalline fluorite was observed only in the Attawapiskat Formation. It occurs as subhedral to euhedral crystals, commonly showing minor dissolution in their cores (Figure GS-14-6). Fluorite partially replaced crinoids, brachiopods, micrite and microspar matrix, and coarse-mosaic calcite cement.

Chalcedony nodules, up to 2.3 mm in diameter, partially replaced crinoid ossicles and crosscut and replaced micrite, microspar and pseudospar matrix in some fossiliferous lithofacies in both formations.

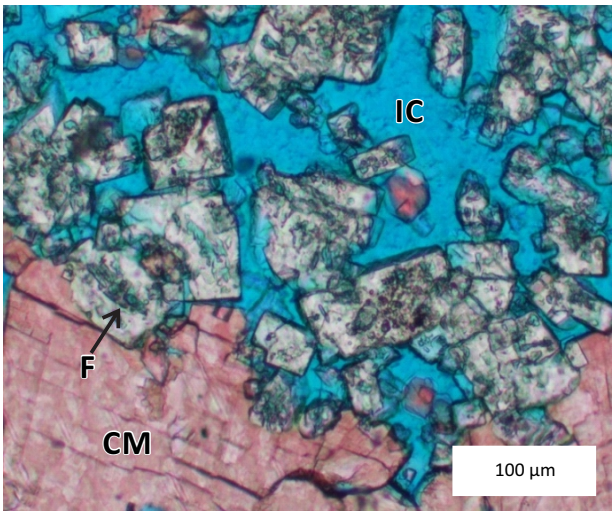

Figure GS-14-6: *Photomicrograph of fluorite (F) partially replacing nonferroan, coarse-mosaic, calcite cement (CM). Blue epoxy highlights intercrystalline porosity (IC). Plane-polarized light. Sample from lithofacies C, Attawapiskat Formation, Merland et al. Whitebear Creek Prov. well at 42.46 m (139.3 ft.). See Figure GS-12-2 (Nicolas et al., GS-12, this volume) for well location.*

Recrystallization and dissolution features

Partial recrystallization of some stromatoporoid, brachiopod, bryozoan, coral and crinoid fragments to coarse crystalline, blocky calcite is very common in fossiliferous lithofacies in both the Ekwan River and Attawapiskat formations. Patchy to pervasive recrystallization (neomorphism) of micrite matrix to microspar or pseudospar is also common. Pinpoint porosity is present within micrite, microspar and pseudospar matrix, as well as lime mudstone intraclasts, in many lithofacies. Vuggy porosity, rarely observed in planar and nonplanar dolomite and within micrite matrix, was filled with isopachous blocky to bladed and coarse-mosaic calcite cements. Moulds of peloids, intraclasts, fragments of gastropods, crinoids, brachiopods, corals and stromatoporoids, and planar-s

and planar-e dolomite rhombs are also present (Figures GS-14-4, -5, -7). Coarse-mosaic calcite cement, filling fractures and vugs, has corroded crystal margins locally. Intracrystalline porosity, in the form of dissolved rims or cores of zoned rhombs in planar-e and planar-s dolomite, was observed in the Ekwan River Formation.

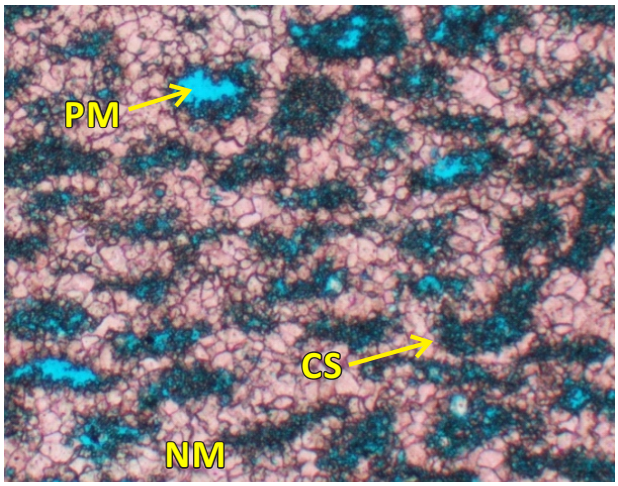

Figure GS-14-7: *Photomicrograph of peloid moulds (PM), 'canoe'-shaped peloids (CS) and neomorphosed (microspar to pseudospar) matrix (NM). Plane-polarized light. Sample from lithofacies D, Ekwan River Formation, Merland et al. Whitebear Creek Prov. well at 69.07 m (226.6 ft.). See Figure GS-12-2 (Nicolas et al., GS-12, this volume) for well location.*

Fractures and compaction features

Fractures and compaction features are common in both the Ekwan River and Attawapiskat formations. Fractures typically crosscut micritic matrix or allochems and are variably occluded by isopachous, fine to coarse crystalline, blocky and coarse-mosaic calcite cement. Rarely, lime mudstone intraclasts are significantly fractured, with those fractures filled by coarse-mosaic calcite cement. Intraclasts, grapestones, ooids and peloids in some lithofacies are typically compacted, forming fitted-grain fabrics. A notable example in the Ekwan River Formation is compacted peloids (now moulds), in peloidal wackestone (lithofacies D), that are oblong to canoe-shaped (Figure GS-14-7). As expected, microstylolites and stylolites are common in both formations.

Interpretation of diagenesis

Paragenetic sequence

The paragenetic sequences of the Ekwan River and Attawapiskat formations have been interpreted separately on the basis of petrographic observations of the textural re-lationships and CL and epifluorescence characteristics of the different diagenetic features. Comparison of these paragenetic sequences reveals striking similarities, indicating that the two formations likely shared similar diagenetic histories. The combined paragenetic sequence for both formations is summarized in Figure GS-14-8 and the justification for this interpretation is provided below; the numbered points correspond to those in Figure GS-14-8.

Marine diagenesis

The marine diagenetic realm comprises the seafloor and shallow marine subsurface, which are characterized by seawater of normal salinity and temperature (James and Choquette, 1983).

1) Allochems are rarely rimmed by micrite cement and isopachous radial-fibrous calcite cement. The latter is, in turn, rimmed by radiaxial-fibrous to radiaxial-blocky calcite cement in some intervals in the Ekwan River Formation. These cements are similar to those reported in previous studies and are typically interpreted to have formed during synsedimentary marine diagenesis (James and Choquette, 1983).

   The margins or interiors of some allochems have been altered to micrite, destroying the original microstructure. These micrite envelopes and micritized allochems are commonly attributed to microborings by marine organisms (Bathurst, 1966; James and Choquette, 1983).

Burial diagenesis

Gradual burial of sediments results in alteration processes related to elevated temperatures and pressures and changing pore-water composition, which characterize the burial or subsurface diagenetic realm (Choquette and James, 1987).

2) Dolomicrite is interpreted to have formed early, as evidenced by the small crystal sizes and its limited occurrence in intertidal and supratidal lithofacies; however, its timing relative to other early diagenetic features is difficult to determine. Replacement of micrite by dolomicrite is commonly interpreted to have occurred in the very shallow burial environment (refer to 'Mechanisms for dolomite formation' section).

   Anhydrite laths crosscut micrite matrix, allochems and radiaxial-fibrous calcite cement. These laths commonly have inclusions of micrite and are clearly replacive in nature. Partial replacement of carbonate sediments by anhydrite laths in this way is commonly interpreted to occur under very shallow burial conditions (Shearman and Fuller, 1969; Dworkin and Land, 1994). The relationship of anhydrite laths to dolomicrite in this study cannot be determined.

3) Early dissolution features include corroded margins of radiaxial-fibrous calcite cement (Ekwan River Formation only) and pinpoint and vuggy porosity

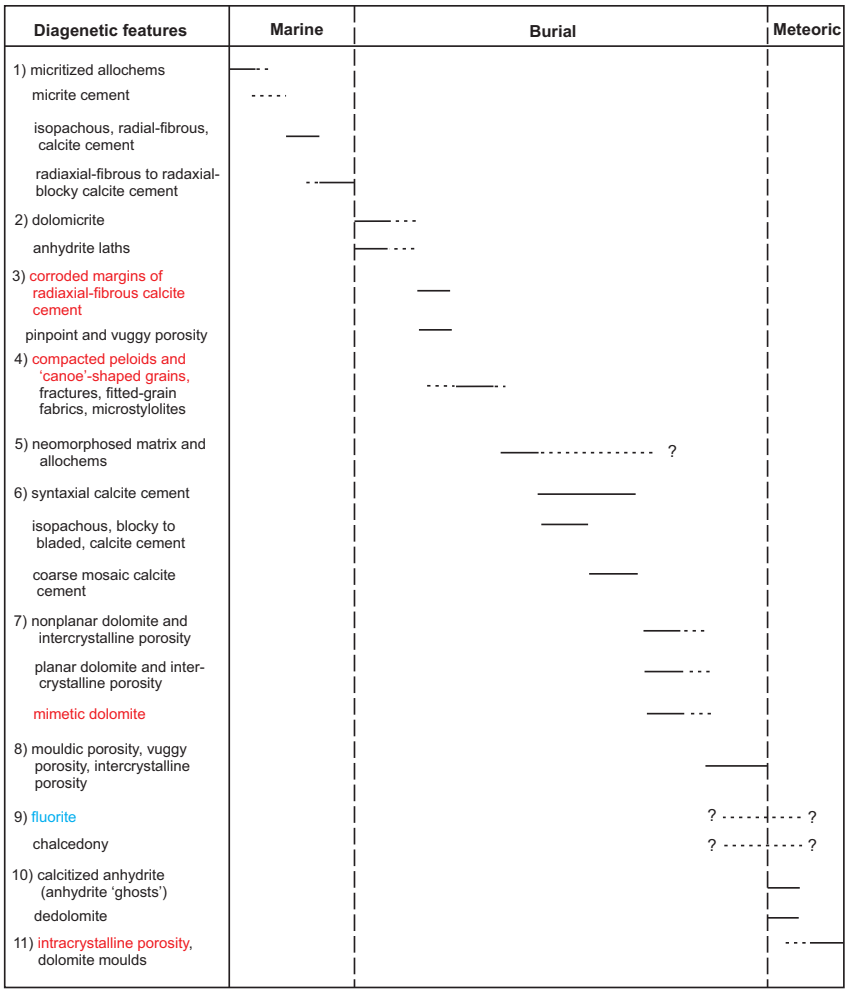

Figure GS-14-8: *Combined paragenetic sequence of the Ekwan River and Attawapiskat formations in the marine, burial and meteoric diagenetic realms. Black text indicates features observed in both formations, red text indicates features observed only in the Ekwan River Formation, and blue text indicates features observed only in the Attawapiskat Formation.*

in micrite matrix. Partial dissolution of peloids in the Ekwan River Formation (later forming canoe-shaped grains) and anhydrite laths in both formations is also interpreted to have occurred at this time. Anhydrite laths that crosscut skeletal allochems were preferentially affected, leaving laths within micrite matrix intact. This stage of dissolution occurred prior to further calcite cementation and dolomitization.

4) Features related to physical compaction include flattened and canoe-shaped peloids (Ekwan River Formation only) and fitted-grain fabrics. Physical compaction was accompanied by minor pressure solution at grain-to-grain contacts in fitted-grain fabrics and the formation of microstylolites, which crosscut micrite matrix and allochems. Compaction occurred after some dissolution of allochems, as shown by the formation of canoe-shaped peloids in which part of each peloid had to be dissolved in order to form the canoe, but before neomorphism, burial calcite cement formation, and dolomitization, as discussed below. However, compaction likely continued on over an extended period of time within the burial realm (Choquette and James, 1987).

5) Neomorphism of allochems and micrite matrix is interpreted to have occurred after the initial compaction of peloids, as there is no evidence of compacted microspar or pseudospar, and prior to more pervasive dissolution of allochems (and formation of peloid moulds). The exact timing of neomorphism is somewhat difficult to determine, but it is generally considered to have initiated during shallow burial (James and Choquette, 1987).

6) Syntaxial calcite overgrowths, isopachous blocky to bladed calcite cements, and coarse-mosaic calcite cements occur together. Isopachous blocky to bladed cement formed first, rimming allochems and lining interparticle and intraparticle pores, anhydrite moulds, vugs and fractures. Coarse-mosaic cement then filled the remaining pore space. Syntaxial overgrowths and isopachous blocky to bladed calcite

cements likely began forming at about the same time, as evidenced by pores where isopachous cements on non-echinodermal allochems and syntaxial overgrowths on echinoderm fragments occur adjacent to each other. These cements also share similar CL and epiflourescence features. Rarely, vugs and intraparticle pores are fully filled by coarse-mosaic cement. These three cements are interpreted to be early burial in origin on the basis of their crystal morphology and relationship to dissolution, compaction and dolomite features (cf. Choquette and James, 1987).

7) Typically, planar dolomite preferentially replaced micrite matrix and, rarely, it partially replaced brachiopods, peloids, intraclasts, neomorphosed matrix, blocky to bladed calcite cement, and coarse-mosaic calcite cement. Based on these relationships, planar dolomite is interpreted to have formed during burial, after an initial dissolution event, compaction, recrystallization and calcite cementation. In most cases, nonplanar dolomite preferentially replaced micrite matrix, and rarely mimetic dolomite partially replaced echinoderm fragments, but the lack of clear crosscutting relationships makes the timing of formation of these dolomites difficult to determine. Nonplanar and planar dolomites, however, are petrographically similar and have similar CL and epiflourescence characteristics, suggesting that they formed at the same time. Mimetic dolomite is tentatively interpreted to have formed at the same time as these dolomites based on their close association, but was only seen in the Ekwan River Formation. Dolomitization resulted in formation of minor intercrystalline porosity. Mechanisms for dolomitization are discussed below.

8) A second stage of dissolution during burial generated crinoid and brachiopod moulds; partially dissolved coral, stromatoporoid and gastropod fragments; and created vuggy and pinpoint porosity. Rare intercrystalline porosity is related to corrosion of coarse-mosaic calcite cement in interparticle spaces, vugs and fractures. Flattened peloids and canoe-shaped peloids were likely partially or fully dissolved to form moulds at this stage of dissolution, as evidenced by minor corrosion of microspar and pseudospar adjacent to peloid moulds and dolomite rhombs within peloid moulds. This dissolution-related porosity remained open.

9) Fluorite rarely replaced skeletal allochems, micrite and neomorphosed matrix, and coarse-mosaic calcite cement (Attawapiskat Formation only). Crosscutting relationships indicate that genesis of fluorite occurred during the later stages of burial diagenesis, roughly coincident with the second stage of dissolution. Salas et al. (2007) suggested that fluorite may precipitate during uplift and cooling or in the deep burial setting due to mixing of hot formation fluids with cooler fluids of a different salinity. Both mechanisms are commonly linked to dolomitization, carbonate dissolution and co-precipitation of fluorite and quartz. For the Attawapiskat Formation, mixing of waters with different salinities in the deep burial environment may be the primary mechanism of fluorite precipitation; however, the presence of later meteoric features (discussed in the following section) suggests that cooling and uplift is also a plausible mechanism. The source of fluorine enrichment is unknown for this study area, but may be from volcanic or fluvial sources, or from shale (cf. Cook et al., 1985; Salas et al., 2007).

Crosscutting relationships indicate that chalcedony formation in the Ekwan River and Attawapiskat formations occurred during late burial diagenesis, after neomorphism and calcite cement precipitation. Its relationship to dolomite is difficult to ascertain, as no crosscutting relationships were observed. Fluid mixing is commonly suggested as a mechanism of chalcedony precipitation (Hesse, 1990). Chalcedony replacement is tentatively linked to fluorite precipitation, and is possibly related to co-precipitation either during mixing of fluids in the deep burial environment or during uplift and cooling, as discussed above (cf. Salas et al., 2007).

Meteoric diagenesis

The meteoric diagenetic realm is characterized by the presence of freshwater, which is typically CO_2-rich, and includes the undersaturated vadose and saturated phreatic zones (James and Choquette, 1984). Meteoric diagenesis of marine deposits may occur relatively early, associated with falling relative sea-level and progressive sedimentation, or during late-stage uplift and/or unroofing of buried carbonate rocks.

10) Anhydrite ghosts and dedolomite are some of the latest diagenetic features noted in this study. The anhydrite ghosts are similar to the products of anhydrite calcitization, as described by Shearman and Fuller (1969) and Kendall (2001). Original gypsum laths were initially replaced by aggregates of anhydrite, which were subsequently replaced by an interlocking mosaic of calcite crystals, strongly resembling microspar and pseudospar. Shearman and Fuller (1969) considered anhydrite calcitization to occur during very early burial, immediately after anhydrite formation. More recent work by Kendall (2001), however, proposed that anhydrite calcitization could occur at a much later stage, in a near-surface environment after uplift. The latter agrees with the interpreted timing of the anhydrite ghosts in the Ekwan and Attawapiskat formations.

Dedolomite formed by the dissolution of rhombs in planar dolomite and subsequent precipitation of nonferroan calcite in their place. This process is tentatively interpreted to occur in the near-surface environment, and may be related to late-stage meteoric diagenesis (cf. Evamy, 1967; Kenny, 1992).

11) Intracrystalline porosity in planar dolomite and dedolomite (Ekwan River Formation only), and planar dolomite moulds indicate that late-stage dissolution took place after dedolomitization. This interpretation is similar to that of Smonsa et al. (2005), who tentatively attribute intracrystalline dolomite porosity to late-stage meteoric diagenesis.

Late-stage meteoric diagenesis of the Ekwan River and Attawapiskat formations is tentatively linked to extensive subaerial exposure of the Hudson Bay Platform during late Silurian to early Devonian time, which resulted in the formation of a significant unconformity surface within the Kenogami River Formation (which overlies the Attawapiskat Formation; Lavoie et al., 2013).

Mechanisms for dolomite formation

Based on core, petrographic and stable-isotope data, Ramdoyal (2012) has proposed two models for dolomitization of the Attawapiskat Formation: the sabkha model and seepage-reflux model. The strong textural and morphological similarities between the Attawapiskat and Ekwan River formations dolomite suggest that these models can be applied to both formations. The sabkha model is the most likely dolomitization model for dolomicrite, on the basis of the fine crystal size of the dolomicrite and its primary occurrence in intertidal and supratidal lithofacies. As the result of gypsum precipitation in the sabkha, Mg^{2+} is concentrated with respect to Ca^{2+} (Morrow, 1982a). The dense brines percolate downwards to as far as 3 m in depth and travel laterally seaward. As they migrate through the sediment, these brines induce the replacement of calcite by dolomite.

The seepage-reflux model has been suggested for the formation of burial dolomites, as supported by the textural characteristics and crosscutting relationships observed in this study, as well as the isotopic data available for the Attawapiskat Formation in Ramdoyal (2012). In this model, concentrated Mg^{2+}-rich brines percolate downwards from an evaporitic lagoon and move laterally toward the ocean; these fluids can reach up to 1000 m in depth (Morrow, 1982b). The overlying evaporites of the Kenogami River Formation may be a possible source of these enriched brines (Lavoie et al., 2013).

Economic considerations

The Hudson Bay Platform is considered to be one of the few frontier basins left in Canada, and as such is of great interest for research into both the stratigraphic and sedimentological characteristics of the strata. In particular, the Ekwan River and Attawapiskat formations have been identified as two of the most likely reservoir units in the succession (Hamblin, 2008; Lavoie et al., 2013). Both are relatively understudied, and are cored in only a few wells. A more detailed understanding of the diagenetic history of these formations allows a better understanding of the processes that most strongly affected the reservoir qualities of these units. Of particular note are the multiple dissolution and dolomitization events that generated high secondary porosity, and the lack of late-stage cementation to occlude this porosity; these processes resulted in reservoir quality increasing with progressive diagenesis. Furthermore, oil staining was observed in intercrystalline porosity in lithofacies E (laminated dolomudstone) in the Ekwan River Formation (Figure GS-14-9), indicating that oil had passed through these formations in the past, and suggesting that there is potential for trapped oil accumulations within the Hudson Bay Basin.

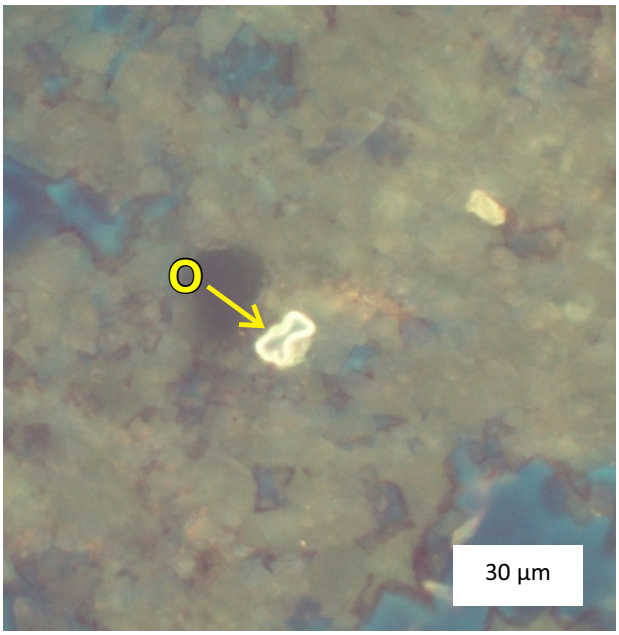

Figure GS-14-9: *Photomicrograph of hydrocarbons (O) rimming an intercrystalline pore. Epifluorescence. Sample from lithofacies E, Ekwan River Formation, Sogepet Aquitaine Kaskattama Prov. No. 1 well at 395.11 m (1296.3 ft.). See Figure GS-12-1 (Nicolas et al., GS-12, this volume) for well location.*

Acknowledgments

The authors would like to thank M.P.B. Nicolas from the Manitoba Geological Survey, and acknowledge the Geological Survey of Canada for their support of this study through phase 2 of the Geo-mapping for Energy and Minerals program.

References

Bathurst, R.G.C. 1966: Boring algae, micrite envelopes and lithification of molluscan biosparites; Geological Journal, v. 5, no. 1, p. 15–32.

Choquette, P.W. and James, N.P. 1987: Limestones – the burial diagenetic environment; Geoscience Canada, v. 14, p. 3–35.

Choquette, P.W. and Pray, L.C. 1970: Geologic nomenclature and classification of porosity in sedimentary carbonates; American Association of Petroleum Geologists Bulletin, v. 54, no. 2, p. 207–244.

Cook, D.J., Randazzo, A.F. and Sprinkle, C.L. 1985: Authigenic fluorite in dolomitic rocks of the Floridan aquifer; Geology, v. 13, p. 390–391.

Dickson, J.A.D. 1965: A modified technique for carbonates in thin section; Nature, v. 205, no. 4971, p. 587.

Dworkin, S.I. and Land, L.S. 1994: Petrographic and geochemical constraints on the formation and diagenesis of anhydrite cements, Smackover Sandstones, Gulf of Mexico; Journal of Sedimentary Research, v. A64, no. 2, p. 339–348.

Evamy, B.D. 1967: Dedolomitization and the development of rhombohedral pores in limestones; Journal of Sedimentary Petrology, v. 37, no. 4, p. 1204–1215.

Folk, R.L. 1965: Some aspects of recrystallization in ancient limestones; *in* Dolomitization and Limestone Diagenesis, L.C. Pray and R.C. Murray (ed.), Society of Economic Paleontologists and Mineralogists, Special Publication 13, p. 14–48.

Hamblin, A.P. 2008: Hydrocarbon potential of the Paleozoic succession of the Hudson Bay/James Bay: preliminary conceptual synthesis of background data; Geological Survey of Canada, Open File 5731, 12 p.

Hesse, R. 1990: Silica diagenesis: origin of organic and replacement cherts; *in* Diagenesis, I.A. McIlreath and D.W. Morrow (ed.), Geoscience Canada, Reprint Series 4, p. 253–276.

James, N.P. and Choquette, P.W. 1983: Limestones – the seafloor diagenetic environment; Geoscience Canada, v. 10, p. 159–179.

James, N.P. and Choquette, P.W. 1984: Limestones – the meteoric diagenetic environment; Geoscience Canada, v. 11, p. 161–194.

Kendall, A.C. 2001: Late diagenetic calcitization of anhydrite from the Mississippian of Saskatchewan, western Canada; Sedimentology, v. 48, p. 29–55.

Kendall, A.C. and Tucker, M.E. 1973: Radiaxial fibrous calcite: a replacement after acicular carbonate; Sedimentology, v. 20, p. 365–389.

Kenny, R. 1992: Origin of disconformity dedolomite in the Martin Formation (Late Devonian, northern Arizona); Sedimentary Geology, v. 78, no. 1–2, p. 137–146.

Lavoie, D., Pinet, N., Dietrich, J., Zhang, S., Hu, K., Asselin, E., Chen, Z., Bertrand, R., Galloway, J., Decker, V., Budkewitsch, P., Armstrong, D., Nicolas, M., Reyes, J., Kohn, B.P., Duchesne, M.J., Brake, V., Keating, P., Craven, J. and Roberts, B. 2013: Geological framework, basin evolution, hydrocarbon system data and conceptual hydrocarbon plays for the Hudson Bay and Foxe basins, Canadian Arctic; Geological Survey of Canada, Open File Report 7363, 210 p.

Morrow, D.W. 1982a: Diagenesis 1. Dolomite – part 1: the chemistry of dolomitization and dolomite precipitation; Geoscience Canada, v. 9, no. 1, p. 5–13.

Morrow, D.W. 1982b: Diagenesis 2. Dolomite – part 2: models and ancient dolostones; Geoscience Canada, v. 9, no. 2, p. 94–107.

Pietrus, E. 2013: Sedimentological analysis and petroleum reservoir potential of the Hudson Bay Basin, northeastern Manitoba; B.Sc. (Honours) thesis, University of Manitoba, Winnipeg, Manitoba, 73 p.

Ramdoyal, A. 2012: Lithofacies analysis, diagenesis and petroleum reservoir potential of the Lower Silurian Attawapiskat Formation, Hudson Bay Basin, northeastern Manitoba; B.Sc. (Honours) thesis, University of Manitoba, Winnipeg, Manitoba, 124 p.

Ramdoyal, A., Nicolas, M.P.B. and Chow, N. 2013: Lithofacies analysis of the Silurian Attawapiskat Formation in the Hudson Bay Lowland, northeastern Manitoba; *in* Report of Activities 2013, Manitoba Mineral Resources, Manitoba Geological Survey, p. 144–155.

Salas, J., Taberner, C., Esteban, M. and Ayora, C. 2007: Hydrothermal dolomitization, mixing corrosion and deep burial porosity formation: numerical results from 1-D reactive transport models; Geofluids, v. 7, p. 99–111.

Shearman, D.J. and Fuller, J.G. 1969: Anhydrite diagenesis, calcitization, and organic laminites, Winnipegosis Formation, Middle Devonian, Saskatchewan; Bulletin of Canadian Petroleum Geology, v. 17, no. 4, p. 496–525.

Sibley, D.F. and Gregg, J.M. 1987: Classification of dolomite rock textures; Journal of Sedimentary Petrology, v. 57, no. 6, p. 967–975.

Smonsa, R., Bruner, K.R. and Riley, R.A. 2005: Paleokarst and reservoir porosity in the Ordovician Beekmantown dolomite of the Central Appalachian Basin; Carbonates and Evaporites, v. 20, no. 1, p. 50–63.